

PerCache: Predictive Hierarchical Cache for RAG Applications on Mobile Devices

Kaiwei Liu¹, Liekang Zeng¹, Lilin Xu², Bufang Yang¹, Zhenyu Yan¹

¹The Chinese University of Hong Kong, ²Columbia University

Abstract

Retrieval-augmented generation (RAG) has been extensively used as a *de facto* paradigm in various large language model (LLM)-driven applications on mobile devices, such as mobile assistants leveraging personal emails or meeting records. However, due to the lengthy prompts and the resource constraints, mobile RAG systems exhibit significantly high response latency. On this issue, one promising approach is to reuse intermediate computational results across different queries to eliminate redundant computation. But most existing approaches, such as KV cache reuse and semantic cache reuse, are designed for cloud settings and perform poorly, overlooking the distinctive characteristics of mobile RAG.

We propose PerCache, a novel hierarchical cache solution designed for reducing end-to-end latency of personalized RAG applications on mobile platforms. PerCache adopts a hierarchical architecture that progressively matches similar queries and QKV cache to maximize the reuse of intermediate results at different computing stages. To improve cache hit rate, PerCache applies a predictive method to populate cache with queries that are likely to be raised in the future. In addition, PerCache can adapt its configurations to dynamic system loads, aiming at maximizing the caching utility with minimal resource consumption. We implement PerCache on top of an existing mobile LLM inference engine with commodity mobile phones. Extensive evaluations show that PerCache can surpass the best-performing baseline by 34.4% latency reduction across various applications and maintain optimal latency performance under dynamic resource changes.

1 Introduction

Emerging deployments of large language models (LLMs) [1, 2, 4, 22, 38, 48, 50, 56, 59] have sunk to various mobile platforms, driving numerous mobile applications such as personal assistants and mailing helpers [9, 10, 33, 42, 46]. An example in Figure 1 shows that such applications often use retrieval-augmented generation (RAG) [30] to generate responses based on personal data from the user’s mobile devices. By deploying both the LLM and personal database locally on mobile devices, these mobile RAG applications can prevent sensitive data leakage and reduce communication latency [33]. However, the prompts containing the retrieved personal data

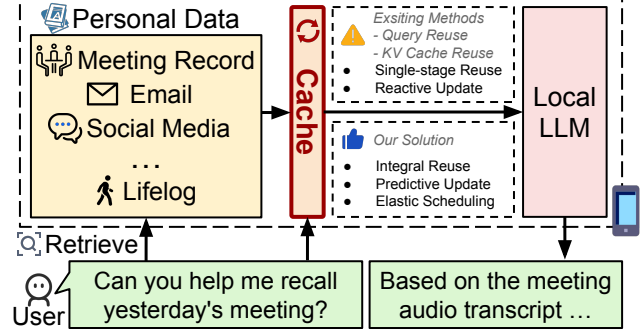


Figure 1: Workflow of mobile RAG applications.

are often extremely lengthy, which can be more than 10 \times of used tokens than the original query [26], resulting in significant computational overhead and response latency, hindering their usability in applications requiring timely responses. For instance, a meeting assistant that needs to quickly retrieve and summarize historical meeting information during an ongoing meeting cannot afford such delays.

To accelerate RAG workflows, prior works have explored the following ways: (1) Model optimization, such as knowledge distillation [5, 8], reduces model size and computational cost in RAG workflows. However, these methods introduce additional retraining overhead and suffer from degraded model performance. (2) Hardware exploitation [35, 43] accelerates RAG workflows through specialized hardware architectures. However, relying on specific hardware design undermines their generalizability and requires complex scheduling mechanisms. (3) RAG retrieval optimization [24, 25, 42, 46, 65] focuses on reducing the latency of knowledge retrieval but cannot address the LLM inference latency caused by long prompts, which constitutes the primary bottleneck in single-user mobile RAG scenarios.

To address this gap, in this work, we focus on the primary latency bottleneck in **mobile** RAG applications: LLM inference. Our observations show that it is possible to share intermediate computational results within the mobile RAG workflows across different user queries. Thus, we consider accelerating mobile RAG workflows by caching reusable results to avoid repeated computation. Some prior works, such as RAGCache [26] and PromptCache [16], reuse the key-value or attention state tensors across different queries to skip portions of attention computation during the prefilling stage.

Other works, such as GPTCache [3] and MeanCache [15], reuse the LLM outputs of previous queries that shows high semantic similarities with the new queries to skip inference. However, these methods are limited to reusing results at a single stage. KV cache reuse can accelerate prefilling, but fails to avoid redundant computation caused by highly similar outputs in the decoding stage. Semantic cache cannot reduce the latency for cache-miss queries even if their prompts contain identical retrieved knowledge texts in the RAG workflow. For mobile RAG, the limitations of single-stage reuse are exaggerated as mobile devices have limited parallel computing capabilities, causing both prefilling and decoding stages to contribute significantly to overall latency. Moreover, single-user mobile RAG applications typically receive much sparser queries than multi-user server applications, making it difficult to populate the cache adequately. This sparsity leads to low cache hit rates and limited efficiency gains.

In this paper, we explore a novel cache system to reduce end-to-end response latency for personalized mobile RAG applications. It effectively leverages reusable results at multiple stages within the RAG pipeline across different queries, achieving high cache hit rates even with sparse user queries. Realizing this goal faces multiple challenges. *First*, it requires fully utilizing the reusable results from each stage to maximize the end-to-end latency reduction. *Second*, we need a new cache population mechanism to improve cache hit rates for single-user mobile RAG applications with sparse query patterns. The reactive population mechanisms adopted by existing solutions make cache hit rates entirely dependent on the received queries. The new mechanism needs to minimize this dependence while improving the hit rate. *Finally*, since mobile devices have severely limited and dynamic computational and storage resources, PerCache must be able to adapt its cache storage and population strategy to effectively utilize system resources without affecting performance.

To this end, we design PerCache, a cache framework to reduce response latency for personalized mobile RAG applications. PerCache adopts a hierarchical cache architecture that stores both query-answer pairs and QKV caches of retrieved knowledge chunks. This design enables comprehensive reuse of intermediate results across mobile RAG workflow stages while providing enhanced flexibility through multiple cache layers. To improve cache hit rates when sparse user queries fail to adequately populate the cache, PerCache employs a query prediction mechanism that predicts future user queries based on knowledge content and historical queries, enabling predictive cache population during device idle time. PerCache also includes a cache scheduler to manage the cache population strategy and the conversion between QA bank and QKV cache tensors, enabling PerCache to effectively utilize dynamically available computational and storage resources while maintaining optimal latency performance.

We implement PerCache on top of mllm [58] and evaluate it using the RAG QA datasets of 20 users from the two public and two self-collected datasets on mobile phones. Experiment results show that PerCache outperforms all baselines, improving hit rate for QKV cache and QA bank by up to 37.56% and 13.8%, respectively, and achieving end-to-end latency reduction by up to 34.4%. We also develop three micro-benchmarks to assess the system’s adaptability under varying resource constraints. The results demonstrate that PerCache can elastically bypass portions of the cache population, reducing computational overhead by 14.12%, and can optimize latency through cross-layer cache conversion.

In summary, this paper makes the following contributions:

- We propose the first predictive hierarchical caching solution designed to reduce response latency for personalized RAG applications on mobile platforms.
- We design a query prediction mechanism that leverages query history and personal data content to predict future user queries, enabling predictive cache population to improve hit rates despite sparse real user queries.
- We analyze latency-computation and latency-storage trade-offs in the cache system. Based on this analysis, we design a cache scheduler that manages the cache population strategy and controls cross-layer cache conversions to effectively utilize dynamically available system resources while maintaining latency performance.
- An implementation and comprehensive evaluation of PerCache show that PerCache outperforms all baselines, achieving up to 34.4% latency reduction while exhibiting strong adaptability to dynamic mobile system resources.

2 Background and Motivation

2.1 Mobile LLM Inference with RAG

LLMs have demonstrated remarkable capabilities across numerous tasks, such as question answering (QA) [63]. Many researchers explore deploying small LMs on mobile platforms [14, 52, 53, 58, 60–62]. Compared to cloud deployment, mobile deployment effectively reduces data transmission latency and protects personal data. The development of retrieval-augmented generation (RAG) [30] further enhances LLM capabilities by enabling LLMs to generate high-quality responses using external knowledge [23].

To improve RAG efficiency, researchers have explored the reuse of intermediate results across queries to avoid redundant computation. Some studies reuse KV cache or attention states of frequently retrieved documents [16, 26, 55], while others cache previously processed queries and their answers [3, 12, 15, 32, 40] or compressed document summaries [12]. However, these approaches narrowly focus on reusing results at individual stages and omit query sparsity in single-user scenarios, leading to suboptimal performance

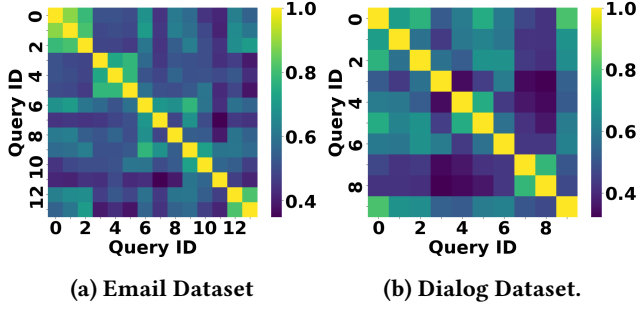


Figure 2: Pairwise semantic similarity of queries from two distinct users in the Email and Dialog datasets.

in **mobile** RAG applications. Section 2.2 and 2.3 present these issues in detail and clarify the goal of our system.

2.2 Reusable Results in Mobile RAG

We identify two types of reusable results in mobile RAG: similar user queries and repeatedly retrieved knowledge.

Similar User Queries. Some queries of individual users are highly semantically similar. We conduct a motivation study using two applications where the LLM serves as a mobile assistant answering questions based on personal daily dialog and email messages, respectively (see Section 5.2 for dataset details). For these two datasets, we recruit separate groups of volunteers: one group uses portable microphones to record their daily dialogues, which are then transcribed into text, while the other group provides their personal emails. For each dataset, volunteers log their queries and the corresponding answers when accessing their dialogue transcripts or emails. We analyze two users, each randomly selected from one dataset, measuring the pairwise semantic similarities among each user’s queries. The results in Figure 2 show that some queries exhibit high semantic similarities. For instance, for the user from the Email dataset, Query₁₂ (“*When will the presentation rehearsal take place?*”) and Query₁₃ (“*Is time of presentation rehearsal given?*”) show a similarity score of 0.815. This indicates the potential to cache historical queries and skip LLM inference for highly similar future queries.

Repeatedly Retrieved Knowledge. In mobile RAG applications, LLMs answer queries based on personal data, where the same knowledge chunks in the personal database may be retrieved repeatedly by different queries. Compared to multi-user RAG applications using public knowledge like Wikipedia, personal knowledge bases on mobile platforms are much smaller and more focused in content scope. Moreover, individual users exhibit consistent language patterns, making repeated retrieval more likely. As shown in Figure 3, we measure the retrieval frequency of knowledge chunks for each user by retrieving the top-2 relevant knowledge chunks per query and recording how often each chunk is accessed. The results show that many chunks are retrieved multiple times, particularly in Email dataset, where every

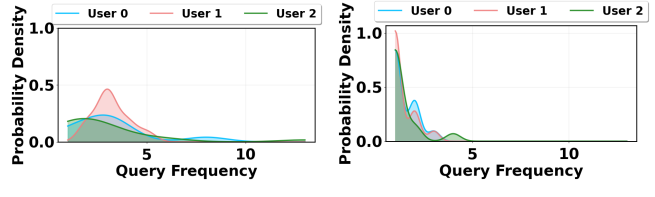


Figure 3: Probability density distribution of knowledge chunk retrieval frequencies.

chunk retrieved by User₁ is retrieved more than once. Such repeated retrieval leads to substantial computational redundancy, as identical intermediate results, such as the KV cache, are repeatedly generated during LLM inference. A natural idea to mitigate this is to store the intermediate results of these repeatedly retrieved chunks for future reuse.

Although there exist reusable results at different stages of mobile RAG, *existing caching solutions only target individual stages in isolation, failing to fully realize the acceleration potential of each stage*. This limitation is demonstrated in Figure 4 through experiments conducted under single-stage caching solutions. We process three user queries from the Email dataset through the RAG pipeline on a mobile phone (Google Pixel 7) and record the LLM pre-filling and decoding latencies for each query. Specifically, Query₁ and Query₂ are semantically similar, while Query₁ and Query₃ are dissimilar but retrieve overlapping knowledge chunks. For Query₁, we additionally record the latencies on a server equipped with an Nvidia RTX A6000 GPU. All experiments use Llama-3.2-3B as the LLM. The results of Query₁ and Query₂ on the mobile phone indicate the limitation of relying solely on KV cache reuse. Although these similar queries retrieve identical knowledge chunks and produce highly similar answers, KV reuse only reduces prefilling latency by skipping KV projection computation and fails to mitigate decoding and other prefilling overheads. The results of Query₁ and Query₃ show the limitation of only reusing similar queries. Although these two queries retrieve overlapping knowledge chunks, Query₃ fails to hit the cache and undergoes full LLM inference. The latency caused by repeatedly retrieved chunks remains unreduced and substantial. These results show that single-stage result reuse is insufficient to reduce the latency caused by computational redundancy. Comparison between the results of Query₁ on server and mobile device reveals a key difference in latency distribution. Unlike server-side inference where decoding dominates the overall latency, mobile inference exhibits significant proportions of both prefilling and decoding latency. This discrepancy primarily stems from the limited parallel computing capabilities of mobile devices. This unique characteristic of mobile devices necessitates the full exploitation of reusable results from each inference stage, which is not achieved by existing approaches.

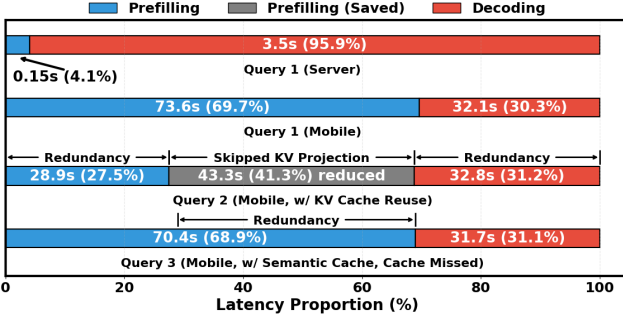


Figure 4: Inference latency breakdown of Llama-3.2-3B on Google Pixel 7 and NVIDIA RTX A6000.

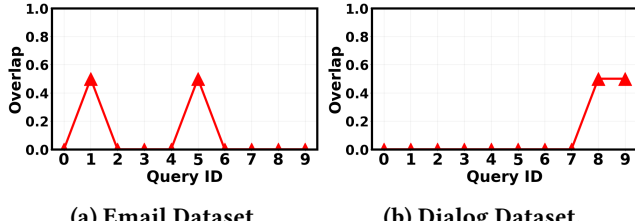


Figure 5: Prefix overlap degree of retrieved chunks.

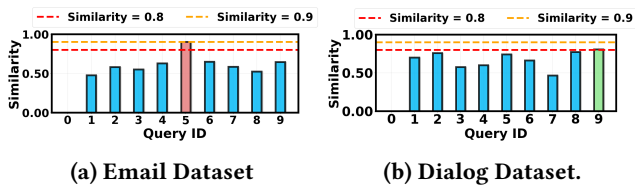


Figure 6: Semantic similarity between each query and its most similar previous query. Query sparsity results in low similarity matches for most queries.

2.3 Sparsity of Single User Query

For mobile RAG applications, the knowledge base stores personal data with only a single user accessing it. However, individual mobile users typically issue queries at a much lower frequency than multi-user RAG systems deployed on centralized servers, and these queries tend to be semantically varied rather than showing significant repetition (Figure 6). **This results in an extremely limited number of queries available for cache population, leading to insufficient cache population and consequently low hit rates.** For example, a user of a personal meeting assistant might only request meeting summaries every few days. Existing methods, including KV cache reuse and semantic cache, reactively update the cache based on received queries, populating new cache entries only upon cache misses. With sparse queries, these approaches struggle to adequately populate the cache in mobile RAG applications, resulting in low cache hit rates.

We illustrate this issue using two cases, corresponding to KV cache reuse and semantic cache, respectively. We use data from one user each in Email and Dialog datasets, sequentially processing all queries and reactively updating

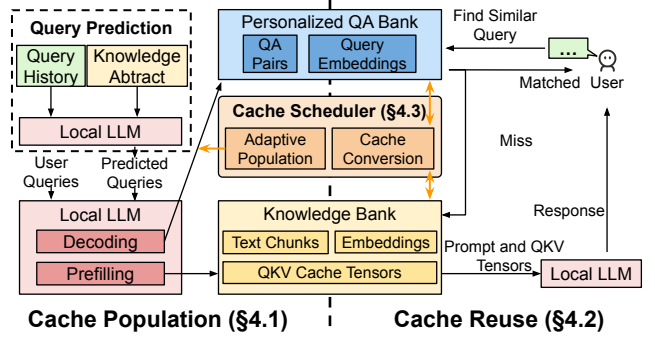


Figure 7: System overview of PerCache.

the cache. As shown in Figure 5, for KV cache reuse (e.g., RAGCache [26]), we retrieve the top-2 relevant knowledge chunks for each query and check their hit rate against cached KV tensors using prefix overlap ratio. The results show that the prefix overlap ratios are quite low for most queries, with some dropping to zero. Similarly, for the semantic cache, we store semantic embeddings of previous queries instead of KV tensors. Figure 6 shows that few queries exhibit high similarity to previously cached queries. For the user from the Email dataset, only Query₅ matches with a similarity above 0.9, while other queries remain below 0.8. These results indicate that the sparsity of single-user queries leads to low cache hit rates with the reactive cache update strategy used by most existing solutions. Although Section 2.2 demonstrates that single-user queries show certain similarities and knowledge chunk retrieval overlap, query sparsity prevents converting these opportunities into significant efficiency gains. Therefore, improving cache hit rates under sparse query frequencies is essential to unlock the efficiency benefits of result reusing in mobile RAG applications.

3 System Overview

Figure 7 overviews the design of our predictive hierarchical cache system, PerCache. The key design principle is to pre-process the partial computational load of the mobile RAG workflow in advance to reduce real-time response latency. PerCache comprises a QA bank, knowledge bank with QKV cache tensors, cache scheduler, and cache prediction module.

The left portion shows the cache population process. There are two layers in PerCache: QA bank and knowledge bank. QA bank stores query-answer pairs and the semantic embeddings of queries, while knowledge bank stores the raw text and embeddings of knowledge chunks and the cached QKV tensors of the chunks retrieved by previous queries. QA bank is designed to match similar queries to directly return cached answers, while QKV tensors are used to skip partial computation in the prefilling stage. To improve hit rate, PerCache adopts an LLM-based query prediction mechanism that predicts future queries to populate cache during device idle time from two views: historical queries and knowledge

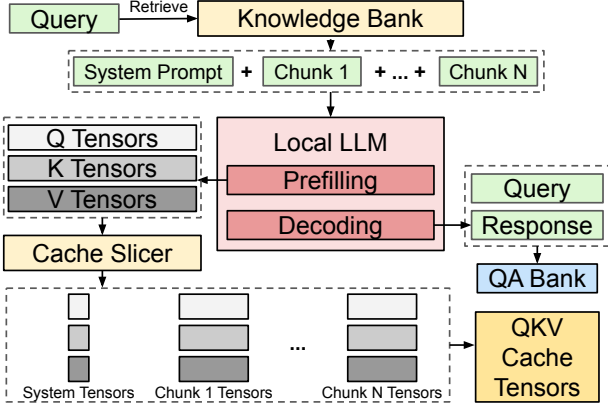


Figure 8: The overflow of cache population.

content. PerCache also includes a cache scheduler to control cache population strategy and conversion between QA bank and QKV tensors, flexibly adapting to dynamically available computational and storage resources.

The right portion illustrates the cache reuse process. Upon receiving a user query, PerCache computes its embedding and compares it with the stored queries in the QA bank. If the highest similarity exceeds the predefined threshold, the cached answer is directly returned, bypassing LLM inference. Otherwise, PerCache retrieves relevant text chunks from the knowledge bank for this query, and checks whether the QKV tensors of each retrieved knowledge chunk are pre-computed and stored in the knowledge bank. These retrieved knowledge chunks are then concatenated with the user query to form the LLM prompt. During the prefilling stage, the computation of the available QKV tensors is skipped. Finally, the LLM output is returned to the user.

4 System Design

This section details each component of PerCache. Section 4.1 describes the hierarchical cache architecture and population process. Section 4.2 explains the details of cache reuse. Section 4.3 presents the design of the cache scheduler.

4.1 Cache Population

Result reusing shows great potential to improve the efficiency of mobile RAG workflows. However, prior methods only consider reusing results at a single stage, which becomes particularly problematic on mobile platforms. They also omit the query sparsity in single-user mobile scenarios that causes a low cache hit rate. For the first issue, we propose a hierarchical cache architecture that caches both query-answer pairs and QKV tensors of the retrieved knowledge chunks to fully exploit reusable results. For the second issue, we predict feature queries to update the hierarchical cache in advance.

4.1.1 Cache Architecture. As shown in Figure 7, the knowledge bank stores the user’s personal data segmented into text chunks with predefined length, along with the semantic embeddings of these chunks. We call each text chunk a *knowledge chunk*. The knowledge bank also stores the QKV tensors for the previously retrieved chunks. When these chunks are retrieved again by future queries, the tensors can be directly loaded to skip Q,K,V projection in the LLM attention module during prefilling. The QA bank stores previously processed queries. It packs each query with its embedding and the answer generated by the LLM as a cache entry.

As shown in Figure 8, the saving of a new QKV cache is triggered by an input query from either the user or the query prediction module (§ 4.1.2). After retrieving relevant knowledge chunks, we concatenate the system prompt, knowledge chunks, and query as input to the LLM. During the prefilling stage, we collect and save the QKV tensors from the attention module of each transformer block. To efficiently utilize the storage space, we adopt the tree structure proposed in [26] to organize the cached QKV tensors of knowledge chunks, where each node represents a specific chunk and each path represents a chunk list retrieved by a specific query. To use the tree structure, we need to save the QKV tensors of each individual chunk in a separate file. To achieve this goal, we implement a cache slicer to split the QKV tensors of the whole prompt into multiple tensor slices. Specifically, the slicer first obtains each chunk’s sequence length using the LLM tokenizer, and then calculates start and end positions of it in the QKV tensors. After that, the slicer splits the QKV tensors into tensor slices on the sequence dimension, each of which corresponds to a single chunk. Each tensor slice is treated as a tree node and merged into the QKV cache tree. We regard the Q, K, V tensor slices of the same chunk as a whole and save them in a single file. In addition to QKV tensors, the QA bank is updated after the decoding stage. Once the LLM output is obtained, the input query, its embedding, and corresponding output are packed into a new cache entry and appended to the QA bank.

Since cache loading latency is typically negligible (Table 1), PerCache loads caches on-demand to minimize memory consumption. The local storage limit for cache is configurable. PerCache allocates a small portion of the total storage (e.g., 100MB) to the QA bank, which is sufficient given the small size of individual entries. PerCache maintains a retrieval count counter for each cached layer and employs the Least Frequently Used (LFU) eviction algorithm to ensure the cache storage does not exceed the configured limit.

4.1.2 Query Prediction. The efficiency gains achieved by the cache system are highly dependent on the cache hit rate. However, existing solutions show suboptimal performance as they only update the cache reactively based on

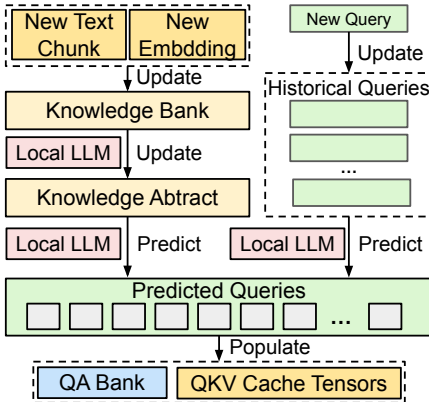


Figure 9: Query prediction with knowledge-based (left) and history-based (right) methods.

user queries. Unlike server-side scenarios, user queries in single-user mobile scenarios are sparse, making it difficult to adequately populate cache, resulting in low cache hit rates.

To address this issue, PerCache predicts the future queries during mobile device idle periods. Idle periods refer to times when users do not interact with their phones for extended durations, such as during overnight or work-hours charging. PerCache utilizes the on-device LLM to infer potential future user queries during these idle periods. The predicted queries are then processed sequentially to update the hierarchical cache using the method described in Section 4.1.1. The number of queries predicted each time is defined as prediction stride, which is a configurable parameter. To comprehensively capture user query patterns, we perform query prediction from two complementary perspectives: knowledge content and query history. For knowledge-based prediction, unlike multi-user RAG systems using diverse public knowledge, mobile RAG applications store domain-specific personal data. For example, email assistant applications rely solely on users' personal emails as external knowledge. Therefore, mobile user queries are usually highly relevant to knowledge content. Through this perspective, the LLM analyzes key contents within the knowledge bank and infers likely future queries around them. For history-based prediction, individual users often show specific linguistic habits and content focus tendencies. This perspective enables the LLM to capture users' questioning patterns and recent shifts in content interests. These two approaches are performed asynchronously.

Specifically, for knowledge-based query prediction, we propose to use knowledge abstracts rather than the raw knowledge chunks for prediction. Raw knowledge chunks are typically lengthy and detailed, making query prediction computationally expensive. In contrast, the knowledge abstract is concise and highly summarized, enabling PerCache to predict queries at a lower computational cost while maintaining a broader view spanning more knowledge chunks. The abstract is a collection of key content from all knowledge

chunks summarized by the LLM. For example, in a meeting memo application, the knowledge bank stores raw audio transcripts of meetings, while the knowledge abstract contains key nouns, important topics, and main participant names. When new knowledge chunks are added into knowledge bank, PerCache notifies the LLM to extract their key content and merge it into the existing abstract. To avoid frequent model loading and inference, PerCache batch-processes multiple chunks to generate abstract when no new chunk arrives for a period, rather than on every incoming chunk. During mobile device idle time, PerCache uses the LLM to infer potential future queries related to the abstract. For history-based query prediction, PerCache maintains a buffer storing recent user queries. If PerCache receives new queries from the user and no additional queries are received within a specified time period thereafter, the history-based prediction is triggered. PerCache first updates the query buffer using these received queries and then instructs the LLM to predict future queries, mimicking the user's expression style and topical interests. Unlike knowledge bank-based prediction, history-based prediction focuses on user query characteristics. By combining knowledge bank-based and history-based prediction, PerCache predicts queries more comprehensively from two complementary views. Since new chunks and queries arrive sparsely and PerCache uses batch processing to predict query, the query prediction module incurs minimal overhead.

4.1.3 Dynamic Cache Refresh. When new personal data is added to the knowledge bank, existing QA pairs may become outdated. To handle this, we implement a cache refresh module. Specifically, PerCache calculates semantic similarities between new chunks and queries in the QA bank. If new chunks rank in the top- $k_{refresh}$ for any query, the corresponding QA pair is updated accordingly.

4.2 Cache Reuse

In this section, we present two mechanisms in PerCache for reducing LLM response latency: QA bank-based similar query reuse and knowledge bank-based QKV cache reuse.

4.2.1 Similar Query Reuse. Upon receiving a user query, PerCache attempts to match it with similar queries in the QA bank. By reusing cached responses from the QA bank, PerCache can skip both prefilling and decoding, enabling near-instantaneous responses for highly similar queries. Specifically, PerCache employs an on-device text embedding model to convert the query into an embedding and computes the cosine similarity with all previously stored queries. If the highest similarity exceeds the similarity threshold τ_{query} , the response in the corresponding QA pair is directly returned to the user, while the actual response to the new query will be generated during the device's idle time and stored in the QA bank for future reuse. The similarity threshold τ_{query} can be

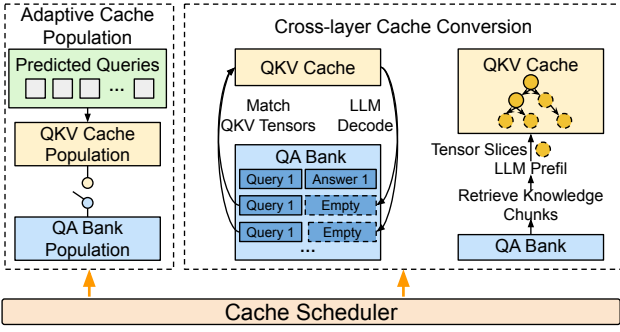


Figure 10: Cache Scheduler.

adjusted to trade off between latency and response quality. A lower threshold increases the QA bank hit rate, allowing more queries to bypass LLM inference. However, setting the threshold too low risks matching queries with low semantic similarity, which may degrade response quality.

4.2.2 QKV Cache Reuse. If the user query fails to match any query in the QA bank, PerCache starts to find the available QKV tensors. Specifically, it first retrieves relevant chunks from the knowledge bank using the hybrid strategy proposed in [13], which combines the BM25 algorithm [44] with text embeddings. After getting the chunks sorted by relevance scores, PerCache starts to match the available pre-computed QKV tensors of these chunks. PerCache examines whether there exist QKV tensors whose text matches the first knowledge chunk. If such tensors are found, PerCache continues to see if there exist such tensors for the second chunk at the position of an immediate child node in the knowledge cache tree. This process continues sequentially until a mismatch is encountered.

After finding available QKV tensors, PerCache starts the LLM inference. It first loads the matched QKV tensors and then concatenates them in order. It also records the total sequence length of the concatenated tensors to calibrate position embedding. During prefilling, for the input tensor of the attention module within each transformer block, PerCache discards the part corresponding to the loaded QKV tensors and only retains the remaining suffix. Q, K, V projection and position embedding computations are performed only on this retained part, significantly reducing computational overhead. Then, the obtained QKV tensors are concatenated with previously loaded QKV tensors, and the subsequent part of attention module proceeds normally. QKV cache reuse enables efficiency improvements in the prefilling stage when no similar queries are matched in the QA bank.

4.3 Cache Scheduler

Compared to servers, mobile devices face severe constraints in battery life, computing power, and storage capacity, and their available system resources frequently fluctuate. Thus, a mechanism is needed to optimize resource consumption while maintaining performance. To this end, we design a

cache scheduler that enables elastic usage of computational and storage resources.

4.3.1 Trade-off Analysis. We identify two primary trade-offs in PerCache as follows.

Latency-Computation Trade-off. As described in Section 4.1, QKV cache and LLM outputs are stored in the knowledge bank and QA bank, respectively. For a single query, generating a QKV cache entry imposes a higher computational load than only producing a QA bank entry. This is because QKV entries require undergoing both prefilling and decoding for final LLM output, while QA bank entries only need prefilling. Higher computational load leads to more battery consumption of the mobile devices. For this issue, we consider two cache population strategies: (1) populate only the QKV cache layer by performing prefilling alone; (2) populate both QKV cache and QA bank layers by executing both stages. The first strategy reduces computational overhead but increases latency as fewer cache entries are populated in the QA bank. The second strategy lowers latency by populating more QA bank entries but increases computational overhead. Thus, a trade-off exists between cache population, computational cost and average response latency.

Latency-Storage Trade-off. PerCache stores both the QA bank and knowledge bank in the local storage of the mobile device. For the QA bank, storing more QA pairs increases the likelihood that a new query will match previous ones with semantic similarity exceeding the threshold. For the knowledge bank, storing more QKV tensors increases the likelihood of finding pre-computed tensors for retrieved knowledge chunks. Higher hit rates in the two layers respectively increase queries that can skip entire inference and the proportion of computation in the attention module, thereby reducing average latency. Thus, caching more entries enables faster responses but consumes more storage.

4.3.2 Adaptive Cache Population. Considering the trade-offs described above, the cache scheduler dynamically adjusts the cache population strategy to avoid computational overhead that does not yield efficiency gains. As shown in Figure 10, the scheduler switches between the strategies described in Section 4.3.1. It adjusts the population strategy based on the similarity threshold rather than historical hit rates, as query sparsity causes few historical hit rate information with large inter-query gaps that weakly correlates with future hit rates. When the similarity threshold is high, few queries match previous ones, and performing decoding would waste computational resources. In this case, the scheduler selects the first strategy, where PerCache performs only prefilling for predicted queries and populates only the knowledge bank with QKV tensors. These queries are also stored in the QA

bank, but without responses. Conversely, when the similarity threshold is low, more queries are likely to match previous ones, and decoding becomes beneficial. In this case, the scheduler selects the second strategy, where PerCache performs both prefilling and decoding to populate both banks. We define a cutoff similarity threshold $\tau_{\text{scheduler}}$ to guide the scheduler’s decision. By adjusting cache population strategy, PerCache avoids unnecessary computation while maintaining end-to-end latency.

4.3.3 Cross-layer Cache Conversion. To enable elastic utilization of computational and storage resources, we implement a mechanism supporting mutual conversion between the two cache layers, as shown in Figure 10. For the conversion from QKV cache to QA bank, the scheduler checks the QA bank and identifies queries lacking corresponding responses that have not undergone decoding. It performs decoding for them and adds the newly generated responses to the QA bank. This process allows PerCache to populate the QA bank using the previous queries that only undergo decoding without prefilling. Such conversion is typically triggered when the similarity threshold τ_{query} becomes low. For the conversion from QA bank to QKV cache, the scheduler checks if QKV tensors of each QA bank query have been deleted by the cache eviction algorithm and if sufficient storage is available. If so, it performs prefilling for these queries and restores their QKV tensors in the knowledge bank again. This conversion allows PerCache to maximize available storage space utilization under any storage constraints to reduce the prefilling stage latency of future queries. Once cache conversion is turned on, it executes automatically in the idle time.

5 Evaluation

5.1 Implementation

We implement a system prototype using C++ and Python based on mllm [58], a mobile LLM inference engine. We use Ollama [41] to deploy text embedding models and use the BM25 [44] algorithm through the rank_bm25 [6] Python package. The system runs locally within Termux [51]. We evaluate PerCache using two LLMs: Llama-3.2-3B model [39] and Qwen-1.5-1.8B [49]. We obtain text embeddings using Qwen3-Embedding-0.6B [64]. The mobile devices used in our experiments include Google Pixel 7 [18], Redmi K60 Pro [20], Samsung Galaxy S22 Ultra [19] and OnePlus Ace 6 [21].

5.2 Experiment Setup

Datasets. We use 4 datasets in our evaluation. We test PerCache on data from 20 users, involving a total of 275 queries.

- *MISeD* [17]. It comprises meeting transcripts from three distinct domains, along with corresponding question-answer pairs. We use 5 users of this dataset.

- *EnronQA* [45]. It consists of emails with question-answer pairs across different user inboxes. We use 5 users of it.
- *Email (Self-collected)*. We recruit 6 volunteers. Over a three-day period, each time they open their email inbox, they record the information they wanted to query and the corresponding answer. We collect all emails from these volunteers along with their real-world query-answer pairs.
- *Daily Dialog Transcript (Self-collected)*. We recruit 4 volunteers to capture their daily conversational speech transcription data over a one-week period via a microphone. The volunteers are allowed to review the transcription data to recall important information and record the corresponding query-answer pairs.

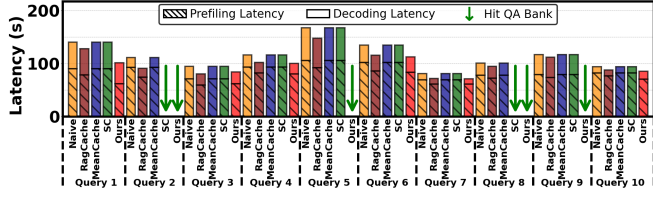
All the self-collected data is collected in the wild without any guideline, ensuring it reflects real-world query patterns.

Baselines. We compare PerCache with following approaches.

- *Naive*. This is the vanilla baseline, where all user queries are processed without any caching mechanisms.
- *RAGCache* [26]. This represents a **KV cache reuse** [16, 26, 55] approach that leverages cached KV tensors during prefilling. It requires the order of the reused KV tensor to match the retrieved knowledge chunk order. RAGCache reactively updates cached KV tensors based on user queries.
- *MeanCache* [15]. This represents a **semantic cache reuse** [3, 15, 32] approach that stores historical queries. MeanCache also reactively updates the cache based on received queries.
- *Sleep-time Compute (SC)* [34]. This represents a **query prediction** approach that infers potential user questions. For this baseline, we select and modify the approach from Sleep-time Compute [34]. The original method predicts questions based on raw context and performs complex reasoning in advance to reduce test-time latency. We adjust it to predict questions and generate answers rather than reasoning processes. For fair comparison, we use the same prompts for query prediction as PerCache.
- *RAGCache + Semantic Meancache*. We create a hierarchical cache baseline manually by combining RAGCache and MeanCache. We employ RAGCache to update KV cache tensor tree and MeanCache to update QA Bank.
- *RAGCache + Sleep-time Compute*. We also create a baseline by combining RAGCache and Sleep-time Compute. We use RAGCache to update the KV cache tensor tree and Sleep-time Compute to update the QA bank.

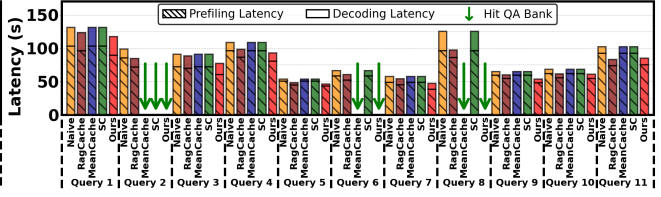
5.3 End-to-end Showcases

To demonstrate the processing details of PerCache, we conduct experiments on two individual users as end-to-end showcases, including one from the MISeD with 10 queries and another from EnronQA with 11 queries. The experiments are conducted in a setting where the target user’s personal data has already been collected and segmented into knowledge chunks before the user queries need to be processed



(a) User₀ in MISED

Figure 11: Inference latency breakdown for each query when all queries from each user are processed sequentially.



(b) User₀ in EnronQA

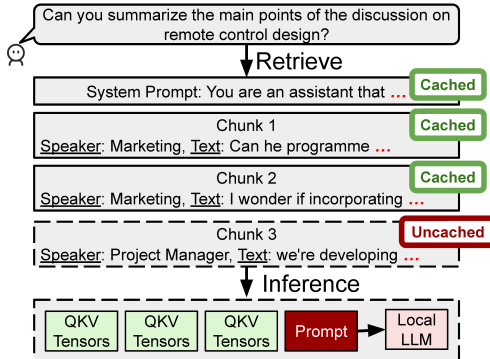


Figure 12: An End-to-end Showcase.

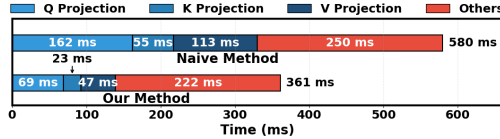


Figure 13: Latency Breakdown of Attention Module.

sequentially. Before processing user queries, PerCache performs knowledge-based query prediction twice, generating five queries each time to populate the cache. After that, user queries are processed one by one. Upon generating the answer for each query, PerCache updates the historical query buffer and performs history-based query prediction, generating five new queries each time to update the cache.

As shown in Figure 11, the latency of each query of PerCache is significantly lower than baselines. On the one hand, PerCache enables more queries to hit the QA bank, with 4 in MISED and 3 in EnronQA, allowing more answers to be returned directly without LLM inference. This improvement stems from the cache population method of PerCache, which predicts queries based on both query history and knowledge content, populating the QA bank more comprehensively. As a result, for each query, more entries in the QA bank exhibit high similarities, increasing the probability of cache hits. On the other hand, for queries that miss the QA bank cache (e.g., Query₁ for both users), PerCache still achieves much lower latency than the baselines. This stems from two factors. First, PerCache's query prediction module can populate more QKV tensors, increasing the hit rate for the knowledge chunks retrieved. Second, unlike RAGCache, which stores only K and V tensors, PerCache also stores Q tensors, skipping more

computation in the attention module. These results indicate that, through its hierarchical architecture, PerCache performs layer-by-layer cache matching, thereby maximizing reuse of intermediate results in mobile RAG workflows. Besides, with query prediction, PerCache improves hit rates for both QA bank and QKV cache layers.

To further show the effectiveness of PerCache, a detailed analysis for Query₁ of User₀ from MISED is demonstrated in Figure 12. Specifically, PerCache retrieves three relevant knowledge chunks for this query and concatenates these chunks, placing a system prompt before the first chunk to clarify the task objective for the LLM. After that, PerCache checks the knowledge bank and finds that the QKV tensors of the system prompt are already cached, and those of the first two chunks have been precomputed using queries predicted by the query prediction module. These tensors, together with the raw text of the third chunk, are packed for LLM inference. As shown in Figure 13, PerCache, with the QKV cache populated by the query prediction module, significantly reduces Q, K, and V projection latencies compared to the naive method. For this query, the latencies of projection decrease by 57.4% (162 → 69 ms), 58.2% (55 → 23 ms), and 58.4% (113 → 47 ms), respectively. This is because the naive method must perform Q, K, and V projections for the system prompt and all three chunks, whereas PerCache only performs for the third chunk.

5.4 Overall Performance

We evaluate PerCache on the 4 datasets: MISED, EnronQA, Email and Dialog. We measure the end-to-end latency for each query and compute the average latency for each user. The number of queries generated per prediction step is set to 5, and the QA bank similarity threshold is fixed at 0.85. Figure 14 demonstrates that PerCache outperforms all baselines, achieving the lowest latency with a 12.55% reduction compared to the best-performing baseline (RAGCache + MeanCache). Especially, for User₀ of MISED dataset, PerCache achieves 51.94% (Naive), 46.21% (RAGCache), 51.94% (MeanCache), 41.16% (Sleep-time Compute), 46.21% (RAGCache + MeanCache) and 34.39% (RAGCache + Sleep-time Compute) latency reduction, respectively. Compared to the naive method, PerCache skips processing queries whose similarities exceed 0.85 and skips Q, K, V projection of the

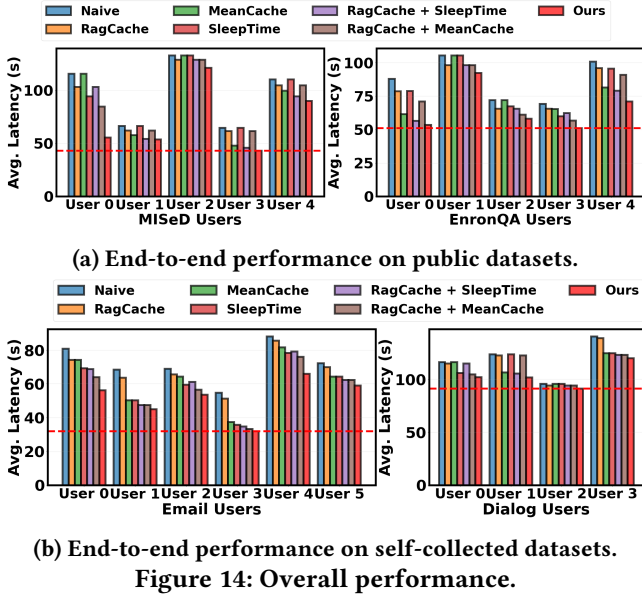


Figure 14: Overall performance.

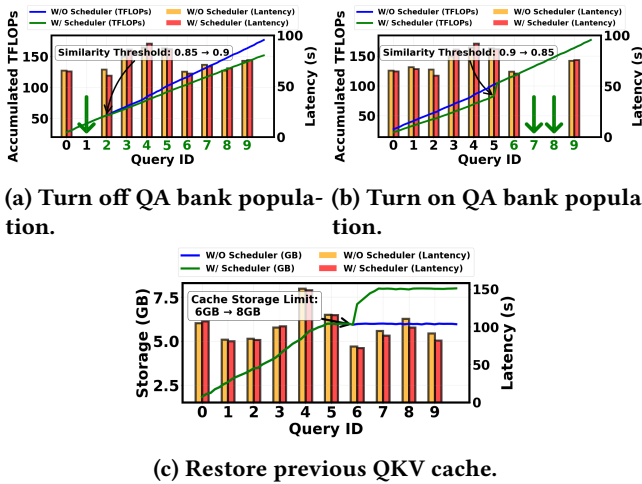


Figure 15: Three cases of cache scheduling.

chunks with pre-computed QKV tensors. Compared to the best-performing “RAGCache + MeanCache” baseline, PerCache achieves higher hit rates for QA bank and QKV cache by leveraging more comprehensive query prediction sources that integrate both historical queries and knowledge bank content for cache population.

5.5 Dynamic Cache Scheduling

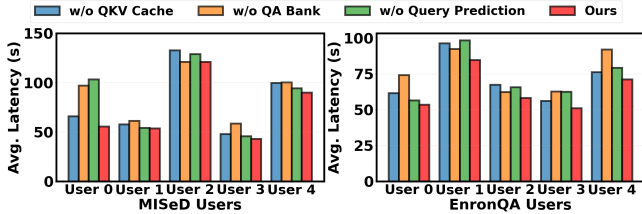
To evaluate the performance of the cache scheduler, we construct three micro-benchmarks under varying dynamic conditions, using the subset of User₀ from the MISeD dataset.

5.5.1 Adaptive Cache Population. Figure 15a illustrates a case where the similarity threshold is raised from 0.85 to

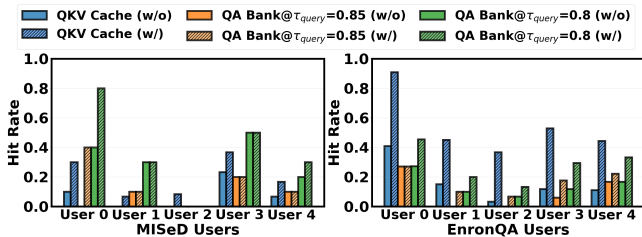
0.90 after Query₂ is processed. Starting from Query₃, the scheduler detects that the threshold surpasses the predefined cutoff, indicating that subsequent queries are unlikely to hit the QA bank. To avoid unnecessary computation on the QA bank population, the scheduler disables LLM decoding for predicted queries and performs only prefilling to update the QKV cache. The green and blue lines in Figure 15a show the accumulated TFLOPs with and without the scheduler, respectively. They indicate that the cache scheduler effectively reduces computational overhead, and the computational savings grow progressively as the cache population proceeds. After processing Query₉, the computational savings reach 14.12% compared to running without the scheduler. Meanwhile, the action of disabling decoding by the scheduler has minimal impact on latency since few user queries hit the QA bank under high similarity thresholds.

5.5.2 Conversion from QKV Cache to QA Bank. In this experiment, we examine a case where the similarity threshold decreases during query processing and analyze the behavior of the scheduler. As shown in Figure 15b, the threshold drops from 0.90 to 0.85 after processing Query₅. The scheduler detects that the threshold has fallen below the cutoff, meaning the QA bank is more likely to be hit by future queries. To improve the QA bank hit rate, the scheduler then identifies the previous queries that were not decoded and performs decoding for them to populate the QA bank after Query₅. Through this adjustment, the cache scheduler achieves latency comparable to the baseline without a scheduler, which always performs both prefilling and decoding for every query.

5.5.3 Conversion from QA Bank to QKV Cache. During runtime, storage limits are configured for both the QA bank and the QKV cache to control cache storage consumption. Since the QA bank requires significantly less space than the QKV cache, it can store a larger number of items than the corresponding QKV tensors. To prevent the cache system from exceeding the limitation, the QKV tensors can be deleted by the cache eviction algorithm when necessary. When the storage limit is increased, PerCache can restore QKV tensors from the QA pairs stored in the QA bank, thereby improving the QKV cache hit rate. Figure 15c, the storage limit for the QKV cache is relaxed from 6GB to 8GB after processing Query₆, which triggers the conversion from the QA bank to the QKV cache. The results show that PerCache achieves lower latencies than the baseline without a cache scheduler when processing Query₇, Query₈, and Query₉. Specifically, with the cache scheduler, PerCache enable these queries to match QKV tensors of two knowledge chunks, while without it, they only match tensors of one chunk. Thus, the cache scheduler helps skip more computation in the prefilling stage by maximizing the utilization of available storage space.



(a) End-to-end Latency.



(b) Average Hit Rate.

Figure 16: Ablation Study.

5.6 Ablation Study

To evaluate the effectiveness of each component, we compare PerCache against variants that individually exclude the QA bank, QKV cache, or query prediction. With τ_{query} set to 0.85 and a prediction stride of 5, Figure 16a shows that PerCache achieves the lowest average latency, indicating that all components effectively contribute to latency reduction. The combination of QA bank and QKV cache achieves fuller reuse of RAG intermediate results, while query prediction improves cache hit rates under sparse user queries. We also record the hit rates of QKV cache and QA bank with τ_{query} set to 0.85 and 0.8. Figure 16b shows that query prediction significantly improves hit rates for both cache layers. On average, QKV cache and QA bank (at $\tau_{\text{query}} = 0.85$ and 0.8) achieve improvements of 11.63%, 8%, and 10% on MISeD, and 37.56%, 6.78%, and 13.8% on EnronQA, respectively. Notably, the impact varies across users and datasets. For instance, the QKV cache contributes most significantly for User₂ in both the MISeD and EnronQA datasets, while the QA bank is most beneficial for User₁, User₃ and User₄ in MISeD and for User₀, User₃ and User₄ in EnronQA. Query prediction shows the highest contribution for User₀ in MISeD and User₁ in EnronQA. This is because the inner similarities and the overlap degree of retrieved chunks differ across different users.

5.7 Sensitivity Analysis

We evaluate the impact of three system parameters: (1) prediction stride: the number of queries generated per prediction; (2) similarity threshold: the semantic similarity threshold used for matching queries in the QA bank; (3) storage limitation: the maximum storage capacity allocated to the

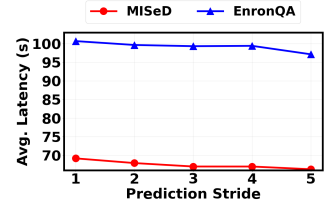


Figure 17: The Impact of Query Prediction Stride.

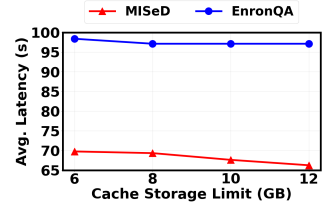
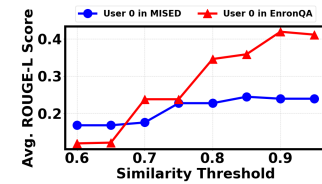
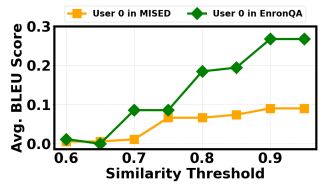


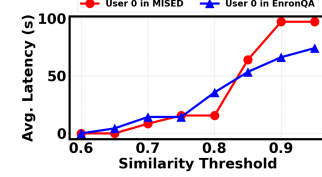
Figure 18: The Impact of Storage Limitation.



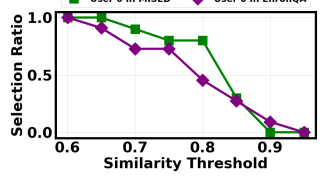
(a) Rouge-L score.



(b) Bleu score.



(c) Average latency.



(d) Hit rate.

Figure 19: Impact of similarity threshold.

cache system. The experiments are conducted on User₀ from the MISeD and EnronQA datasets.

5.7.1 Impact of Prediction Stride. We evaluate the performance of PerCache with the prediction stride ranging from 1 to 5. Figure 17 shows that the average latency slightly decreases as the prediction stride increases. A larger prediction stride enables more QA pairs and QKV cache tensors to be stored in the cache system, which also improves the diversity of predicted queries and their corresponding retrieved knowledge chunks. As a result, the hit rates for both cache layers increase, thereby reducing the inference latency.

5.7.2 Impact of Storage Limitation. To evaluate the impact of storage limitations, we configure storage limitations ranging from 6GB to 12GB. As shown in Figure 18, the average latency decreases as the storage limit increases. This is because, with relaxed storage limitations, fewer QKV tensors are evicted and more tensors are retained in the cache system. Consequently, more retrieved knowledge chunks can match their corresponding QKV tensors.

5.7.3 Impact of Similarity Threshold. To study the effect of the similarity threshold, we vary it from 0.60 to 0.95 and measure the ROUGE-L and BLEU scores of the generated responses, along with the average latency and QA bank hit

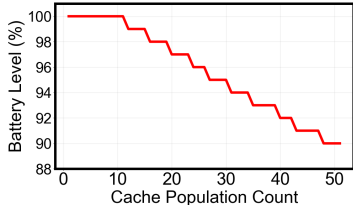


Figure 20: Battery level variation with cache population count using LLama-3.1-3B on OnePlus Ace 6.

rate. As shown in Figure 19, higher thresholds improve generation quality but increase latency and reduce hit rates. This is because higher thresholds lower the number of queries that successfully match entries in the QA bank. As a result, more queries are processed by the LLM instead of reusing potentially mismatched cached responses, which improves generation quality. When queries fail to match, they can only reuse precomputed QKV tensors. These results highlight a trade-off between generation quality and end-to-end latency.

5.8 System Overhead

To evaluate power consumption, we repeatedly execute PerCache’s complete cache population process using a query from User₀ of MISed (349 input tokens, 136 output tokens). Each cache population includes query embedding generation, knowledge chunk retrieval, similar query matching, QKV tensor matching and loading, and saving new QKV tensors and QA pairs. The experiments are conducted using LLama-3.2-3B on OnePlus Ace 6. Figure 20 shows 51 cache population consume 10% battery. In our system, the number of queries for single query prediction is typically set between 1-5, consuming just 1%-2% battery. Moreover, since personal knowledge bases and query histories update infrequently, and PerCache operates during device idle time (configurable to charging-only), practical power consumption remains negligible.

6 Related Work

6.1 Caching for LLM Serving

Numerous works reuse KV cache across different inputs to avoid redundant computation [11, 16, 26, 37, 54, 57, 66, 67]. Prompt Cache [16] achieves structured reuse of attention states for text segments. MobiLoRA [31] reuses the KV cache of shared contexts for LoRA serving on mobile devices. Other works use semantic caching [3, 12, 15, 32, 40] to store historical queries and skip inference for semantically similar new queries. GPTCache [3] uses centralized storage for query-response pairs across all users. MeanCache [15] employs user-specific caches and uses federated learning for privacy-preserving embedding model training. To improve cache hit rate, SCALM [32] uses hierarchical semantic clustering to

identify significant cache entries. However, these approaches adopt a reactive strategy to update the cache based on received user queries, resulting in low hit rate under sparse query patterns in single-user mobile environments.

6.2 RAG Performance Optimization

Significant efforts have focused on the optimization of the performance of the RAG workflow. RAGCache [26] reuses KV cache of external knowledge across multiple requests, computing KV tensors only when absent. Camille et al. [12] cache compressed document summaries for latency reduction. However, these works update cache reactively without considering mobile query sparsity. We address this through query prediction that predictively populates the cache to improve hit rates. There are also some works focusing on the acceleration of the knowledge retrieval process. Chameleon [24] implements a distributed engine for large-scale vector search. PipeRAG [25] proposes to pipeline the retrieval and LLM generation processes to reduce the latency. RaLMSpec [65] stores documents in a local cache and speculatively retrieves documents from this cache, verifying them against the retrieval results from the remote knowledge base. RAGO [23] abstracts the RAG workload in a unified schema and proposes a systematic framework to optimize scheduling policies for RAG workflow. Different from them, we focus on single-user mobile scenarios with one-turn QA, where retrieval latency is not a bottleneck since personal knowledge bases are much smaller than servers and retrieval occurs only once per query.

6.3 Pre-computation for LLM Inference

Pre-computation is a widely adopted strategy for reducing real-time latency in many systems. Sleep-time Compute [34] infer potential user questions and conduct LLM reasoning in advance to reduce test-time inference latency. PROMTEC [29] pre-computes frequently occurring token sequences offline and accelerates online inference by matching and validating candidate sequences from the pre-computed corpus. Pre³ [7] pre-computes deterministic grammar transition mappings to eliminate runtime parsing overhead for structured LLM outputs. Inspired by these works, we predict future user queries and populate the cache based on the predicted results in advance to improve the cache hit rate.

7 Discussion

Compatibility. PerCache can be extended to other Transformer-based LLMs like Gemma [48], which share similar attention mechanisms despite different weight distributions. Future work could also apply PerCache to multimodal models such as LLaVA [36] to support diverse modalities of personal data.

More Flexible Query Prediction. The number of predicted queries of PerCache is currently configured as a system parameter, which may not be the best choice for each query

prediction. Future work will investigate more adaptive approaches that enable the LLM to dynamically determine the appropriate number of queries based on contextual demands. **Fine-grained Cache Organization.** PerCache currently stores complete QKV cache tensors for each retrieved knowledge chunk. Future work can explore more fine-grained cache organization strategies, such as selectively storing different tensor components for different knowledge chunks (e.g., preserving only Q tensors) or caching intermediate states from various positions within the attention module for different chunks (e.g., QKV tensors or attention states).

8 Conclusion

We propose PerCache, a hierarchical cache system for mobile RAG applications. PerCache integrates semantic cache for user queries and QKV cache reuse for retrieved knowledge chunks, fully exploiting reusable results in mobile RAG workflows. It utilizes the local LLM to predict future queries to improve cache hit rates under sparse user queries and enables flexible cache scheduling to adapt to dynamic system resources. PerCache outperforms existing cache solutions with up to 34.4% end-to-end latency reduction.

References

- [1] Marah Abdin, Jyoti Aneja, Harkirat Behl, Sébastien Bubeck, Ronen Eldan, Suriya Gunasekar, Michael Harrison, Russell J Hewett, Mojan Javaheripi, Piero Kauffmann, et al. 2024. Phi-4 technical report. *arXiv preprint arXiv:2412.08905* (2024).
- [2] Loubna Ben Allal, Anton Lozhkov, Elie Bakouch, Gabriel Martín Blázquez, Guilherme Penedo, Lewis Tunstall, Andrés Marafioti, Hynek Kydliček, Agustín Piqueres Lajarín, Vaibhav Srivastav, et al. 2025. SmollM2: When Smol Goes Big-Data-Centric Training of a Small Language Model. *arXiv preprint arXiv:2502.02737* (2025).
- [3] Fu Bang. 2023. Gptcache: An open-source semantic cache for llm applications enabling faster answers and cost savings. In *Proceedings of the 3rd Workshop for Natural Language Processing Open Source Software (NLP-OSS 2023)*. 212–218.
- [4] Marco Bellagente, Jonathan Tow, Dakota Mahan, Duy Phung, Maksym Zhuravinskyi, Reshinth Adithyan, James Baicoianu, Ben Brooks, Nathan Cooper, Ashish Datta, et al. 2024. Stable lm 2 1.6 b technical report. *arXiv preprint arXiv:2402.17834* (2024).
- [5] Yuri Façanha Bezerra and Li Weigang. 2025. Llmquoter: enhancing rag capabilities through efficient quote extraction from large contexts. *arXiv preprint arXiv:2501.05554* (2025).
- [6] Dorian Brown, Vít Starý Novotný, et al. 2022. rank_bm25: A Collection of BM25 Algorithms in Python. https://github.com/dorianbrown/rank_bm25. https://github.com/dorianbrown/rank_bm25 GitHub repository.
- [7] Junyi Chen, Shihao Bai, Zaijun Wang, Siyu Wu, Chuheng Du, Haileong Yang, Ruihao Gong, Shengzhong Liu, Fan Wu, and Guihai Chen. 2025. Pre³: Enabling Deterministic Pushdown Automata for Faster Structured LLM Generation. *arXiv preprint arXiv:2506.03887* (2025).
- [8] Jennifer Chen, Aidar Myrzakhan, Yaxin Luo, Hassaan Muhammad Khan, Sondos Mahmoud Bsharat, and Zhiqiang Shen. 2025. DRAG: Distilling RAG for SLMs from LLMs to Transfer Knowledge and Mitigate Hallucination via Evidence and Graph-based Distillation. *arXiv preprint arXiv:2506.01954* (2025).
- [9] Philipp Christmann and Gerhard Weikum. 2025. Recursive Question Understanding for Complex Question Answering over Heterogeneous Personal Data. *arXiv preprint arXiv:2505.11900* (2025).
- [10] Philipp Christmann and Gerhard Weikum. 2025. The ReQAP System for Question Answering over Personal Information. *arXiv preprint arXiv:2508.06880* (2025).
- [11] Kexin Chu, Tzechinh Liu, Yunding Li, Pengchao Yuan, and Wei Zhang. [n. d.]. CaR: An Efficient KV Cache Reuse System for Large Language Model Inference. ([n. d.]).
- [12] Camille Couturier, Spyros Mastorakis, Haiying Shen, Saravan Rajmohan, and Victor Rühle. 2025. Semantic Caching of Contextual Summaries for Efficient Question-Answering with Language Models. *arXiv preprint arXiv:2505.11271* (2025).
- [13] Leon Eversberg. 2024. How to Use Hybrid Search for Better LLM RAG Retrieval: Building an advanced local LLM RAG pipeline by combining dense embeddings with BM25. *TDS Archive, Medium* (11 August 2024). <https://medium.com/data-science/how-to-use-hybrid-search-for-better-llm-rag-retrieval-032f66810ebe> 11 min read.
- [14] ggml-org. 2023. *llama.cpp: LLM inference in C/C++*. <https://github.com/ggml-org/llama.cpp> GitHub repository with 85.3k stars and 12.8k forks.
- [15] Waris Gill, Mohamed Elidrisi, Pallavi Kalapatapu, Ali Anwar, and Muhammad Ali Gulzar. 2024. Privacy-aware semantic cache for large language models. *CoRR* (2024).
- [16] In Gim, Guojun Chen, Seung-seob Lee, Nikhil Sarda, Anurag Khandelwal, and Lin Zhong. 2024. Prompt cache: Modular attention reuse for low-latency inference. *Proceedings of Machine Learning and Systems 6* (2024), 325–338.
- [17] Lotem Golany, Filippo Galgani, Maya Mamo, Nimrod Parasol, Omer Vandsburger, Nadav Bar, and Ido Dagan. 2024. Efficient Data Generation for Source-grounded Information-seeking Dialogs: A Use Case for Meeting Transcripts. *arXiv preprint arXiv:2405.01121* (2024).
- [18] Google Mobile. 2024. Pixel 7 – Google Mobile. <https://www.google-mobile.cn/?product=pixel-7>. Accessed: 2025-07-27.
- [19] GSMArena. 2022. *Samsung Galaxy S22 Ultra 5G - Full phone specifications*. https://www.gsmarena.com/samsung_galaxy_s22_ultra_5g-11251.php Released 2022, February 25.
- [20] GSMArena. 2023. *Xiaomi Redmi K60 Pro - Full phone specifications*. https://www.gsmarena.com/xiaomi_redmi_k60_pro-12046.php Released 2023, January 01.
- [21] GSMArena. 2025. *OnePlus Ace 6 - Full phone specifications*. https://www.gsmarena.com/oneplus_ace_6_5g-14259.php Accessed: December 5, 2025.
- [22] Shengding Hu, Yuge Tu, Xu Han, Chaoqun He, Ganqu Cui, Xiang Long, Zhi Zheng, Yewei Fang, Yuxiang Huang, Weilin Zhao, et al. 2024. Minicpm: Unveiling the potential of small language models with scalable training strategies. *arXiv preprint arXiv:2404.06395* (2024).
- [23] Wenqi Jiang, Suvinay Subramanian, Cat Graves, Gustavo Alonso, Amir Yazdanbakhsh, and Vidushi Dadu. 2025. Rago: Systematic performance optimization for retrieval-augmented generation serving. In *Proceedings of the 52nd Annual International Symposium on Computer Architecture*. 974–989.
- [24] Wenqi Jiang, Marco Zeller, Roger Waleffe, Torsten Hoefer, and Gustavo Alonso. 2023. Chameleon: a heterogeneous and disaggregated accelerator system for retrieval-augmented language models. *arXiv preprint arXiv:2310.09949* (2023).
- [25] Wenqi Jiang, Shuai Zhang, Boran Han, Jie Wang, Bernie Wang, and Tim Kraska. 2024. Piperag: Fast retrieval-augmented generation via algorithm-system co-design. *arXiv preprint arXiv:2403.05676* (2024).
- [26] Chao Jin, Zili Zhang, Xuanlin Jiang, Fangyue Liu, Xin Liu, Xuanzhe Liu, and Xin Jin. 2024. Ragcache: Efficient knowledge caching for retrieval-augmented generation. *arXiv preprint arXiv:2404.12457* (2024).

[27] László Kozma and Johannes Voderholzer. 2024. Theoretical analysis of byte-pair encoding. *arXiv preprint arXiv:2411.08671* (2024).

[28] Woosuk Kwon, Zhuohan Li, Siyuan Zhuang, Ying Sheng, Lianmin Zheng, Cody Hao Yu, Joseph Gonzalez, Hao Zhang, and Ion Stoica. 2023. Efficient memory management for large language model serving with pagedattention. In *Proceedings of the 29th symposium on operating systems principles*. 611–626.

[29] Alan Chi-Man Lee, Wing-Sun Cheng, and Calvin Chun-Kit Chan. 2025. PROMTEC: Fast LLM Inference Decoding using Prompt Multi-Lookup with Template Database and Common Sequences. In *Findings of the Association for Computational Linguistics: ACL 2025*. 6830–6842.

[30] Patrick Lewis, Ethan Perez, Aleksandra Piktus, Fabio Petroni, Vladimir Karpukhin, Naman Goyal, Heinrich Küttler, Mike Lewis, Wen-tau Yih, Tim Rocktäschel, et al. 2020. Retrieval-augmented generation for knowledge-intensive nlp tasks. *Advances in neural information processing systems* 33 (2020), 9459–9474.

[31] Borui Li, Yitao Wang, Haoran Ma, Ligeng Chen, Jun Xiao, and Shuai Wang. 2025. MobiLoRA: Accelerating LoRA-based LLM Inference on Mobile Devices via Context-aware KV Cache Optimization. In *Proceedings of the 63rd Annual Meeting of the Association for Computational Linguistics (Volume 1: Long Papers)*. 23400–23410.

[32] Jiaxing Li, Chi Xu, Feng Wang, Isaac M von Riedemann, Cong Zhang, and Jiangchuan Liu. 2024. Scalm: Towards semantic caching for automated chat services with large language models. In *2024 IEEE/ACM 32nd International Symposium on Quality of Service (IWQoS)*. IEEE, 1–10.

[33] Yuanchun Li, Hao Wen, Weijun Wang, Xiangyu Li, Yizhen Yuan, Guohong Liu, Jiacheng Liu, Wenxing Xu, Xiang Wang, Yi Sun, et al. 2024. Personal llm agents: Insights and survey about the capability, efficiency and security. *arXiv preprint arXiv:2401.05459* (2024).

[34] Kevin Lin, Charlie Snell, Yu Wang, Charles Packer, Sarah Wooders, Ion Stoica, and Joseph E Gonzalez. 2025. Sleep-time Compute: Beyond Inference Scaling at Test-time. *arXiv preprint arXiv:2504.13171* (2025).

[35] Chaoqiang Liu, Haifeng Liu, Dan Chen, Yu Huang, Yi Zhang, Wenzing Xiao, Xiaofei Liao, and Hai Jin. 2025. HeterRAG: Heterogeneous Processing-in-Memory Acceleration for Retrieval-augmented Generation. In *Proceedings of the 52nd Annual International Symposium on Computer Architecture*. 884–898.

[36] Haotian Liu, Chunyuan Li, Qingyang Wu, and Yong Jae Lee. 2023. Visual instruction tuning. *Advances in neural information processing systems* 36 (2023), 34892–34916.

[37] Yuhan Liu, Hanchen Li, Yihua Cheng, Siddhant Ray, Yuyang Huang, Qizheng Zhang, Kuntai Du, Jiayi Yao, Shan Lu, Ganesh Ananthanarayanan, et al. 2024. Cachegen: Kv cache compression and streaming for fast large language model serving. In *Proceedings of the ACM SIGCOMM 2024 Conference*. 38–56.

[38] Zhenyan Lu, Xiang Li, Dongqi Cai, Rongjie Yi, Fangming Liu, Xiwen Zhang, Nicholas D Lane, and Mengwei Xu. 2024. Small language models: Survey, measurements, and insights. *arXiv preprint arXiv:2409.15790* (2024).

[39] Meta AI. 2024. Llama 3.2: Revolutionizing edge AI and vision with open, customizable models. <https://ai.meta.com/blog/llama-3-2-connect-2024-vision-edge-mobile-devices/>. Accessed: 2025-07-27.

[40] Ramaswami Mohandoss. 2024. Context-based semantic caching for llm applications. In *2024 IEEE Conference on Artificial Intelligence (CAI)*. IEEE, 371–376.

[41] Ollama Team. 2024. Ollama: Get up and running with Llama 3.3, DeepSeek-R1, Phi-4, Gemma 3, Mistral Small 3.1 and other large language models. <https://github.com/ollama/ollama>. <https://github.com/ollama/ollama> GitHub repository.

[42] Taehwan Park, Geonho Lee, and Min-Soo Kim. 2025. MobileRAG: A Fast, Memory-Efficient, and Energy-Efficient Method for On-Device RAG. *arXiv preprint arXiv:2507.01079* (2025).

[43] Derrick Quinn, E Ezgi Yücel, Martin Prammer, Zhenxing Fan, Kevin Skadron, Jignesh M Patel, José F Martínez, and Mohammad Alian. 2025. DReX: Accurate and Scalable Dense Retrieval Acceleration via Algorithmic-Hardware Codesign. In *Proceedings of the 52nd Annual International Symposium on Computer Architecture*. 1108–1124.

[44] Stephen Robertson, Hugo Zaragoza, et al. 2009. The probabilistic relevance framework: BM25 and beyond. *Foundations and Trends® in Information Retrieval* 3, 4 (2009), 333–389.

[45] Michael J Ryan, Danmei Xu, Chris Nivera, and Daniel Campos. 2025. Enronqa: Towards personalized rag over private documents. *arXiv preprint arXiv:2505.00263* (2025).

[46] Korakit Seemakhupt, Sihang Liu, and Samira Khan. 2024. Edgerag: Online-indexed rag for edge devices. *arXiv preprint arXiv:2412.21023* (2024).

[47] Jianlin Su, Murtadha Ahmed, Yu Lu, Shengfeng Pan, Wen Bo, and Yunfeng Liu. 2024. Roformer: Enhanced transformer with rotary position embedding. *Neurocomputing* 568 (2024), 127063.

[48] Gemma Team, Thomas Mesnard, Cassidy Hardin, Robert Dadashi, Surya Bhupatiraju, Shreya Pathak, Laurent Sifre, Morgane Rivière, Mihir Sanjay Kale, Juliette Love, et al. 2024. Gemma: Open models based on gemini research and technology. *arXiv preprint arXiv:2403.08295* (2024).

[49] Qwen Team. 2024. Introducing Qwen1.5. <https://qwenlm.github.io/blog/qwen1.5/>

[50] Qwen Team. 2025. Qwen3-0.6B. <https://huggingface.co/Qwen/Qwen3-0.6B>. Accessed: 2025-08-26.

[51] Termux Contributors. 2025. Termux - a terminal emulator application for Android OS extendible by variety of packages. <https://github.com/termux/termux-app>. GitHub repository, accessed July 2025.

[52] Daliang Xu, Hao Zhang, Liming Yang, Ruiqi Liu, Gang Huang, Mengwei Xu, and Xuanzhe Liu. 2025. Fast on-device LLM inference with npus. In *Proceedings of the 30th ACM International Conference on Architectural Support for Programming Languages and Operating Systems, Volume 1*. 445–462.

[53] Zhenliang Xue, Yixin Song, Zeyu Mi, Xinrui Zheng, Yubin Xia, and Haibo Chen. 2024. Powerinfer-2: Fast large language model inference on a smartphone. *arXiv preprint arXiv:2406.06282* (2024).

[54] Jingbo Yang, Bairu Hou, Wei Wei, Yujia Bao, and Shiyu Chang. 2025. KVLink: Accelerating Large Language Models via Efficient KV Cache Reuse. *arXiv preprint arXiv:2502.16002* (2025).

[55] Jiayi Yao, Hanchen Li, Yuhan Liu, Siddhant Ray, Yihua Cheng, Qizheng Zhang, Kuntai Du, Shan Lu, and Junchen Jiang. 2025. CacheBlend: Fast Large Language Model Serving for RAG with Cached Knowledge Fusion. In *Proceedings of the Twentieth European Conference on Computer Systems*. 94–109.

[56] Yuan Yao, Tianyu Yu, Ao Zhang, Chongyi Wang, Junbo Cui, Hongji Zhu, Tianchi Cai, Haoyu Li, Weilin Zhao, Zhihui He, et al. 2024. Minicpm-v: A gpt-4v level mllm on your phone. *arXiv preprint arXiv:2408.01800* (2024).

[57] Lu Ye, Ze Tao, Yong Huang, and Yang Li. 2024. Chunkattention: Efficient self-attention with prefix-aware kv cache and two-phase partition. *arXiv preprint arXiv:2402.15220* (2024).

[58] Rongjie Yi, Xiang Li, Zhenyan Lu, Hao Zhang, Daliang Xu, Liming Yang, Weikai Xie, Chenghua Wang, Xuanzhe Liu, and Mengwei Xu. 2023. mllm: fast and lightweight multimodal LLM inference engine for mobile and edge devices. <https://github.com/UbiquitousLearning/mllm>

[59] Rongjie Yi, Xiang Li, Weikai Xie, Zhenyan Lu, Chenghua Wang, Ao Zhou, Shangguang Wang, Xiwen Zhang, and Mengwei Xu. 2024. PhoneLM: An efficient and capable small language model family through principled pre-training. *arXiv preprint arXiv:2411.05046*

(2024).

[60] Wangsong Yin, Mengwei Xu, Yuanchun Li, and Xuanzhe Liu. 2024. Llm as a system service on mobile devices. *arXiv preprint arXiv:2403.11805* (2024).

[61] Wangsong Yin, Rongjie Yi, Daliang Xu, Gang Huang, Mengwei Xu, and Xuanzhe Liu. 2024. Elms: Elasticized large language models on mobile devices. *arXiv preprint arXiv:2409.09071* (2024).

[62] Jinliang Yuan, Chen Yang, Dongqi Cai, Shihe Wang, Xin Yuan, Zeling Zhang, Xiang Li, Dingge Zhang, Hanzi Mei, Xianqing Jia, et al. 2024. Mobile foundation model as firmware. In *Proceedings of the 30th Annual International Conference on Mobile Computing and Networking*. 279–295.

[63] Mуронг Yue. 2025. A survey of large language model agents for question answering. *arXiv preprint arXiv:2503.19213* (2025).

[64] Yanzhao Zhang, Mingxin Li, Dingkun Long, Xin Zhang, Huan Lin, Baosong Yang, Pengjun Xie, An Yang, Dayiheng Liu, Junyang Lin, et al. 2025. Qwen3 Embedding: Advancing Text Embedding and Reranking Through Foundation Models. *arXiv preprint arXiv:2506.05176* (2025).

[65] Zhihao Zhang, Alan Zhu, Lijie Yang, Yihua Xu, Lanting Li, Phitchaya Mangpo Phothilimthana, and Zhihao Jia. 2024. Accelerating retrieval-augmented language model serving with speculation. *arXiv preprint arXiv:2401.14021* (2024).

[66] Yilong Zhao, Shuo Yang, Kan Zhu, Lianmin Zheng, Baris Kasikci, Yang Zhou, Jiarong Xing, and Ion Stoica. 2024. Blendserve: Optimizing offline inference for auto-regressive large models with resource-aware batching. *arXiv preprint arXiv:2411.16102* (2024).

[67] Yun Zhu, Jia-Chen Gu, Caitlin Sikora, Ho Ko, Yinxiao Liu, Chu-Cheng Lin, Lei Shu, Liangchen Luo, Lei Meng, Bang Liu, et al. 2024. Accelerating inference of retrieval-augmented generation via sparse context selection. *arXiv preprint arXiv:2405.16178* (2024).

Appendix

A More Evaluation Results

A.1 Performance on Different Mobile Platforms

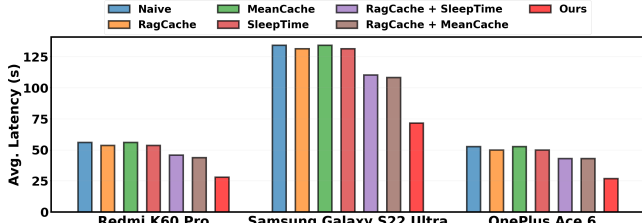


Figure 21: Overall performance comparison on MISed and EnronQA datasets across three mobile devices: Redmi K60 Pro, Samsung Galaxy S22 Ultra, and OnePlus Ace 6.

As shown in Figure 21, to evaluate the performance of PerCache across mobile devices with different hardware configurations, we select a representative user ($User_0$) from the MISed dataset and repeat PerCache along with all baseline methods on Redmi K60 Pro, Samsung Galaxy S22 Ultra, and OnePlus Ace 6. It should be noted that not all devices were brand new, and some may have experienced varying degrees of hardware degradation. The results demonstrate that while all methods exhibit similar trends in latency variation across devices due to different hardware specifications, PerCache consistently achieves the lowest average latency regardless of the device used. This demonstrates that our method does not rely on specific hardware features and maintains consistently superior performance across devices of various performance tiers, proving its robustness. Furthermore, its ability to run on consumer-grade devices across different price ranges indicates broad application potential.

A.2 Performance with Qwen

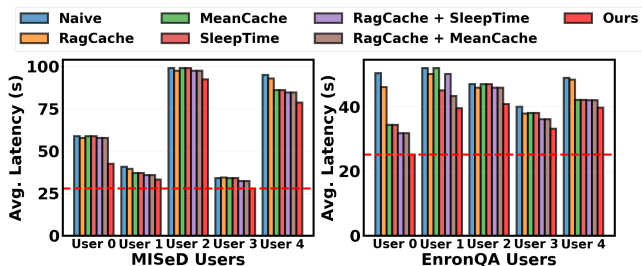


Figure 22: End-to-end performance using Qwen-1.5-1.8B on MISed and EnronQA datasets.

As shown in Figure 22, to evaluate our system’s performance with different on-device LLMs, we replicate the previous experiments using Llama-3.2-3B by modifying the Qwen modeling file in the mllm engine, and then employ Qwen-1.5-1.8B throughout for knowledge abstract generation, query prediction, and final response generation. All other settings remain identical to the previous experiments using Llama-3.2-3B. As illustrated in the figure, our method still maintains the lowest latency among all baselines, with particularly significant improvements observed for $User_0$ on the EnronQA dataset. Due to differences between Qwen-1.5-1.8B and Llama-3.2-3B in model size, prediction capabilities, the proportion of attention-related weights, and certain inference steps, the results differ somewhat from those obtained with Llama-3.2-3B. Nevertheless, our method still demonstrates significant, consistent, and substantial improvements, indicating the generalizability of our approach across different model architectures.

A.3 Generation Quality

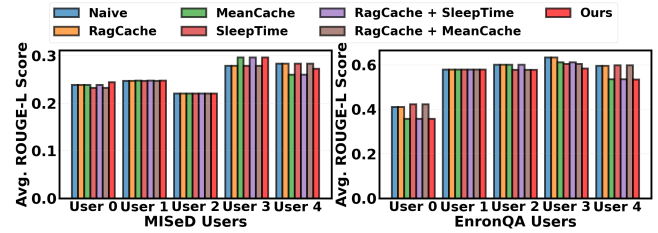


Figure 23: Final answer quality of PerCache on MISed and EnronQA datasets.

As shown in Figure 23, to assess response generation quality, we use the ROUGE-L score as a metric to compare PerCache’s answers with the ground-truth responses. The similarity threshold for QA bank is set to be 0.85. This demonstrates that our method can achieve substantial latency gains while maintaining relatively stable response generation quality.

A.4 System Overhead

Table 1: System Overhead

Latency (s)		Storage / Item	
Operation	Time	Component	Size
Matching Question	1.61	QA Bank	4KB
Knowledge Retrieval	3.94		
Matching QKV Cache	0.015	QKV Cache	87MB
QKV Cache Loading	1.03		
LLM Prefilling	62.14	Knowledge Chunk	16KB
LLM Decoding	10.95		

We measure the latency and storage overhead of each component of PerCache using the queries of $User_0$ from the EnronQA dataset. The prediction stride is set to 5, and the knowledge chunk length is fixed at 100 words. As shown in Table 1, most of the latency comes from LLM prefilling and decoding, which account for 77.9% and 13.7%, respectively. This confirms that PerCache is designed to optimize the primary bottleneck in the pipeline. The results also show that the QKV cache dominates storage consumption with 87MB per chunk. Its space usage can be effectively controlled by configuring the storage limit parameter.

B More Implementation Details

B.1 Inference with QKV Cache

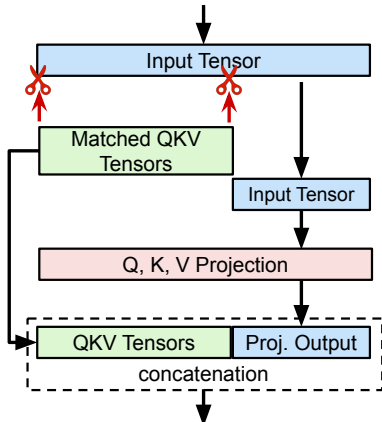


Figure 24: Inference implementation details.

Figure 24 shows a simple implementation diagram of how PerCache uses precomputed QKV Cache for inference acceleration during the prefill phase. The input text is first converted from a string to a tensor by the tokenizer, and then passes through the LLM’s embedding layer. At this point, PerCache loads the previously matched QKV tensor from disk and obtains the sequence length value L_{pre} of the QKV tensor. Meanwhile, it also records the sequence length value L_{total} of the embedding layer’s output. Afterwards, this tensor goes through several transformer blocks. As shown in Figure 24, within each block, the portion of the tensor with sequence length L_{pre} is first cropped from the beginning of the input tensor of that layer, keeping only the latter part. Then, the portion with sequence length $L_{total} - L_{pre}$ is used to perform the QKV projection operation. Subsequently, along the sequence dimension, the loaded QKV tensor is concatenated before the output tensor of the QKV projection. At this point, the sequence length is restored from $L_{total} - L_{pre}$ to L_{total} . The subsequent operations then proceed normally.

It is worth noting that since LLama-3.2-3B and Qwen-1.5-1.8B in the mllm repository use Rotary Position Embedding

(RoPE) [47] for position encoding, we need to make appropriate adjustments accordingly. Specifically, after obtaining the computation results of the QKV projection on the cropped input tensor, we cannot directly apply RoPE position encoding. Instead, we need to adjust the position index used for retrieving the precomputed sine and cosine values. In the implementation, before applying RoPE to the cropped tensor with length $L_{total} - L_{pre}$, we first offset the position counter by adding L_{pre} . This ensures that when accessing the sine and cosine lookup tables, the position encodings correspond to the actual positions in the original full sequence rather than starting from position 0.

B.2 Tokenization Inconsistency

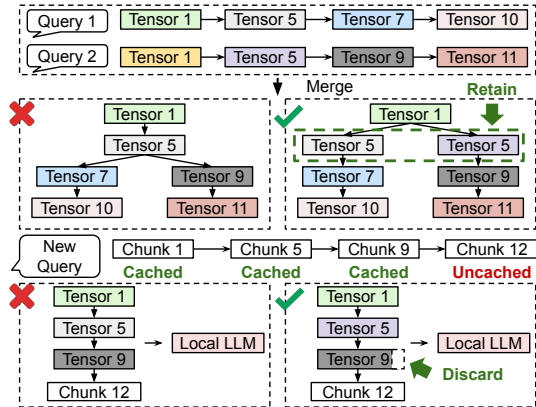


Figure 25: Tokenization inconsistency and solution.

Unlike inference engines such as vLLM [28] that use fixed-size KV blocks as nodes in the cache prefix tree, each node in our QKV cache tree is an individual knowledge chunk, which facilitates the logical management of the QKV cache tree. Additionally, to organize the QKV cache according to the semantic content of knowledge chunks, we perform prefix matching using strings rather than tokens or token hashes. However, we notice that some LLM tokenizers like Byte-Pair Encoding (BPE) [27] may cause subword segmentation inconsistency. As shown in Figure 25, two queries are processed to populate the QKV cache tree. PerCache merges the common prefix of the QKV tensor chains of their retrieved knowledge chunks and integrates the merged binary tree into the overall cache tree. For a new query retrieving chunks 1, 5, 9, and 12, the system loads and concatenates the cached QKV tensors of chunks 1, 5, and 9, then packs the concatenated tensor with chunk 12’s raw text for inference. However, we find that the inference results often differ from naive raw-text-only inference without cache. This is because: (1) The tokenization results near the boundary between tensor 5 (gray) and 7 are different from those between tensor

5 (purple) and 9; (2) The tokenization results at the end of tensor 9 are also different from the results when directly inputting the concatenated text of chunks 9 and 12 into the tokenizer. We take two measures for this issue: (1) When merging QKV cache tensor chains, we retain the last node (tensor 5) of the common prefix and only merge up to the second-to-last node of the common prefix; (2) For a matched tensor chain, we discard tensors of the last few tokens in the final node (tensor 9), using raw text inference for this portion instead.

B.3 Prompt Details

In this section, we provide the prompts used in PerCache.

Knowledge Abstract Generation

Please summarize the following text into a sentence that captures the key events and key concepts: [knowledge chunks]. Focus only on the essential core content and main ideas. Do NOT include any other text or explanations.

Figure 26: Prompt template for knowledge abstract generation.

Figure 26 shows the prompt template designed to enable the local LLM to extract summaries from one or multiple knowledge chunks. To use this template, PerCache simply replaces the [knowledge chunks] slot with the corresponding knowledge chunk(s) from which to extract summaries. Once a summary is generated, it will be appended to the overall summary collection.

Knowledge-based Query Prediction

You are a smartphone AI assistant that helps users by checking their [personal emails/daily dialog/meeting record] to answer questions. Here is some abstract of the content: [knowledge abstract].

Think about what questions users are most likely to ask regarding this content in their daily life.

The user might ask two kind of questions about their [personal emails/daily dialog/meeting record], such as:

1. General questions. Such as "What is the main topic of the [personal emails/daily dialog/meeting record] recorded on XXX?".
2. Detailed questions. Such as "What activities did the user mention doing on XXX day?".

Now guess [prediction step] questions that users might ask. Provide them in this format: '1. ...?; 2. ...?; 3. ...?' without any other text or explanations.

Figure 27: Prompt template for knowledge-based query prediction.

Figure 27 shows the prompt template used for knowledge-based query prediction. PerCache replaces the [knowledge abstract] slot with the corresponding knowledge abstracts, the [personal emails/daily dialog/meeting record] slot with the type of external knowledge base, and the [prediction step] slot with the number of queries to predict. This template guides the LLM to generate two types of questions: general questions and detail-oriented questions, aiming to cover a comprehensive range of question types.

History-based Query Prediction

You are a smartphone AI assistant that helps users by checking their [personal emails/daily dialog/meeting record] to answer questions. Here is their recent query history: [query history].

Generate another [prediction step] questions users might ask. Carefully analyze and mirror the language style, tone, formality level, and interests shown in the examples.

Please provide them in this format: '1. ...?; 2. ...?; 3. ...?' Do not repeat the examples. Do not include any other text or explanations, just the questions.

Figure 28: Prompt template for history-based query prediction.

Figure 28 shows the prompt template used for history-based query prediction. When using this template, PerCache replaces the [query history] slot with queries from the query history buffer, the [personal emails/daily dialog/meeting record] slot with the type of external knowledge base, and the [prediction step] slot with the number of queries to predict. This template guides the local LLM to predict future queries by mimicking the language style, tone, formality level, and interests of real user queries.